Endohedral Metalloborofullerenes $La_2@B_{80}$ and $Sc_3N@B_{80}$: A Density Functional Theory Prediction†

Peng Jin,‡,§ Ce Hao,‡,* Zhanxian Gao,‡ Shengbai B. Zhang,⊥ and Zhongfang Chen§,*

State Key Laboratory of Fine Chemicals, Dalian University of Technology, Dalian, 116024, P.R. China, Department of Chemistry, University of Puerto Rico, San Juan, Puerto Rico 00931, Department of Physics, Applied Physics, and Astronomy, Rensselaer Polytechnic Institute, Troy, New York 12180

Received: March 4, 2009; Revised Manuscript Received: May 13, 2009

The geometries, electronic and spectroscopic properties of two representative endohedral derivatives of B_{80} fullerene, namely, $La_2@B_{80}$ and $Sc_3N@B_{80}$, and the possibility for their production were investigated by means of density functional computations. The very favorable binding energies suggest a considerable possibility to experimentally realize these novel endohedral metalloborofullerenes. Infrared absorption spectra and ^{11}B nuclear magnetic resonance spectra were also computed to assist future experimental characterization.

1. Introduction

Endohedral metallofullerenes (EMFs) are novel materials enclosing a variety of metal atoms in fullerene cages.[1] The possibility of tuning physical and chemical properties depending on the nature of the encapsulated atoms may aid searches for materials with the right potential for electronic, optical, or magnetic applications. Interestingly, substantial charge transfer from the enclosed metal atoms to the outer frameworks has a ubiquitous feature in EMFs. The transferred electrons not only change the electronic structures of fullerenes, but also can help stabilize the unstable fullerene species, which violate the well-known isolated pentagon rule (IPR)[2] and the pentagon adjacency penalty rule.[3] Consequently, a series of non-IPR fullerene cages have been experimentally synthesized or theoretically predicted by encaging different types of metal atom(s). Some such examples are $Sc_2@C_{66}$,[4] $Sc_3N@C_{68}$,[5] $Sc_2C_2@C_{68}$,[6] $Sc_3N@C_{70}$,[7] $La@C_{72}$,[8] $La_2@C_{72}$,[9] $Ce_2@C_{72}$,[10] $DySc_2N@C_{76}$,[11] $Dy_3N@C_{78}$ (II),[12] $Gd_3N@C_{82}$,[13] $M_3N@C_{84}$ (M = Tb,[14] Tm and Gd[15]). These findings remarkably enriched the carbon fullerene family.

Herein, we turn to the element boron. Boron has one less valence electron than its neighbor carbon. Due to its electron deficiency, boron requires triangulated polyhedra (deltahedra), which are held together by two-center−two-electron (2c−2e) B−B bonds and three-center−two-electron (3c−2e) B−B−B bonds to form boron clusters.[16] Apparently, fullerene cages with only pentagons and hexagons are not feasible for element boron.

A recent fascinating density functional theory (DFT) study by Szwacki et al.[17] predicted a fullerene-like hollow cage composed of 80 boron atoms. By adding 20 extra boron atoms to the centers of all hexagons of a truncated icosahedral B_{60} cage, they obtained an energetically more favored B_{80}, which was named boron fullerene or boron buckyball. Holding a large cohesive energy of 5.76 eV/atom, B_{80} fullerene has a great possibility for experimental production.[17] Although B_{80} with high I_h symmetry suggested by Szwacki et al. was not a local minimum and spontaneously breaks down to T_h symmetry,[18] it resembles the electronic property of C_{60} very well.[19]

B_{80} fullerene can be wrapped by a planar boron sheet. Inspired by the B_{80} fullerene structure with triangular and hexagonal motifs, the most stable α boron sheet was proposed[20,21] and considered as the precursor of B_{80}.

Other B_{80}-based materials were also proposed by means of DFT computations. B_{80} can condense into stable solid forms (i.e. fcc and bcc B_{80}) with some distortions.[22,23] B_{80} fullerene could be a good media for hydrogen storage by being doped with some alkali metals (Li, Na, K).[24] Remarkably, a large boron fullerene family, including some new members with even higher stability than B_{80}, was predicted.[19a,25] All these show us an exciting future for boron chemistry.

According to the work of Szwacki et al.,[17] B_{80} has an inner cavity with a diameter of about 8.17 Å, comparable to that of the C_{80} (I_h). B_{80} is also a promising electron receptor and prefers to accommodate six extra electrons, due to its low-lying 3-fold degenerate LUMO orbitals and rather large electron affinity (3 eV).[18c] The similarities between B_{80} and C_{80} (I_h) in terms of cavity sizes and electronic structures remind us of EMFs with C_{80} (I_h) outer cages, such as $La_2@C_{80}$[26] and $Sc_3N@C_{80}$.[27] Therefore, it is very interesting to explore if some metal atoms or clusters can be encapsulated into the B_{80} cage to form endohedral species. These novel structures could be named *endohedral metalloborofullerene*. Once synthesized, they may have extensive applications in a variety of fields, such as chemistry and electromagnetic and biomedical science. For instance, as a boron-rich cluster, they may be employed for boron neutron capture therapy.

In this study, we investigated the structures and electronic and spectroscopic properties of two representative B_{80}-based endohedral complexes, $La_2@B_{80}$ and $Sc_3N@B_{80}$, by means of DFT computations. The highly aromatic B_{80} hexaanion cages are good hosts to encage metal atom(s) and clusters to form endohedral species. With large binding energies, the endohedral complexes such as $La_2@B_{80}$ and $Sc_3N@B_{80}$ are promising for experimental production. Infrared spectra and ^{11}B NMR (nuclear magnetic resonance) spectra were computed for these novel endohedral complexes to assist future experimental characterization.

† Part of the "Walter Theil Festschrift".

* To whom correspondence should be addressed. E-mails: haoce@dlut.edu.cn (C.H.); zhongfangchen@gmail.com (Z.C.).

‡ Dalian University of Technology.

§ University of Puerto Rico.

⊥ Rensselaer Polytechnic Institute.

10.1021/jp9019848 CCC: $40.75
Published on Web 07/16/2009

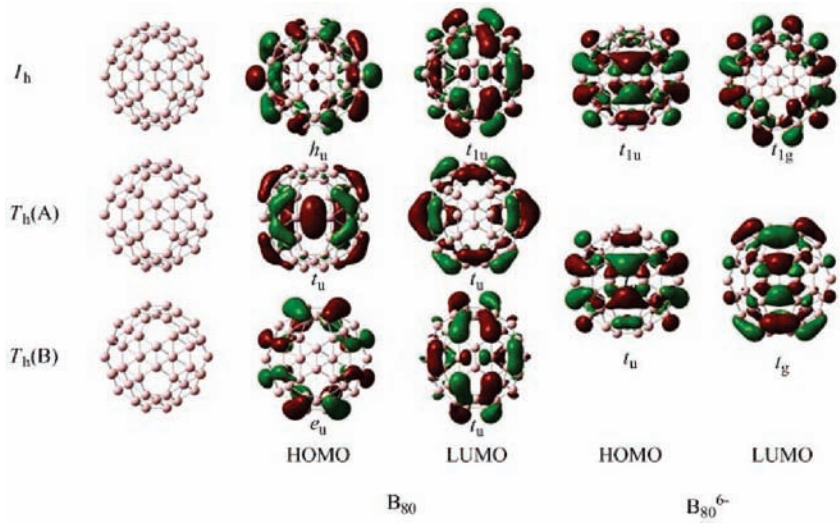

Figure 1. Geometries and frontier orbitals of the three B_{80} isomers and their hexaanions.

2. Computational Methods

The Gaussian 03 software package was employed throughout our DFT computations.[28] Full geometry optimizations with symmetry constraints for the B_{80} isomers and their hexaanions were carried out using the B3LYP functional[29] with the 6-31G* basis set.[30] For endofullerenes ($La_2@B_{80}$ and $Sc_3N@B_{80}$), the 3-21G basis set for B, N, and Sc atoms[31] and a double-ζ basis set (LanL2DZ) with the effective core potential for La[32] (denoted here by 3-21G∼dz) were used. All endohedral geometries were characterized by harmonic vibrational frequency analysis at the same theoretical level after the optimization.

Electron affinities and ionization potentials were computed at the B3LYP/6-31G*∼dz theoretical level for the lowest-energy isomers. Nucleus-independent chemical shifts (NICS, in ppm),[33,34] a simple and efficient method to evaluate aromaticity, were computed at the cage centers of the optimized B_{80} fullerenes. The NICS values for the empty B_{80} cages and the ^{11}B NMR spectra for the lowest-energy endohedral isomers were computed using the gauge-independent atomic orbital method[35] at the B3LYP/6-31G*∼dz theoretical level. The ^{11}B NMR chemical shifts were first calculated by using B_2H_6 as internal standard (absolute shift $\sigma = 93.5$) then were referenced to $BF_3 \cdot OEt_2$ (δ (B_2H_6)16.6 vs $BF_3 \cdot OEt_2$). We also computed the ^{11}B chemical shift of $B_4(^tBu)_4$ using the current scheme; the δ value is 145.5 ppm (experiment: 135.4 ppm).[36]

To evaluate the feasibility of producing endohedral fullerenes experimentally, we computed the binding energy (E_b) at the B3LYP/6-31G*∼dz level of theory. E_b is defined as the difference between the total energy of an endofullerene and the sum of total energies of the separated empty B_{80} cage and encapsulated atoms (i.e., $E_b = [E_{tot}(B_{80}) + E_{tot}(M)] - E_{tot}(M@B_{80})$).

3. Results and Discussion

3.1. B_{80} Isomers and Their Hexaanions. We considered three B_{80} isomers with high symmetry (namely, I_h, T_h (A), and T_h (B) (Figure 1)) following the literature findings.[17,18] These three isomers have very close thermodynamic stabilities (energy differences <1.0 kcal/mol) and similar HOMO−LUMO gap energies (ca. 1.9 eV), and T_h (B) is energetically the most favorable (Table 1). Our results support previous reports.[18b,c,19b] Apparently, all three isomers have low-lying 3-fold degenerate LUMOs (Figure 1), which enable them to accommodate six extra electrons, similar to carbon fullerenes.[37]

TABLE 1: Computed Relative Energies (E_{rel}, kcal/mol), HOMO−LUMO Gap Energies (eV), and Nuclear Independent Chemical Shifts (NICS) of the Three B_{80} Isomers and Their Hexaanions at the B3LYP/6-31G* Level of Theory

	B_{80}			B_{80}^{6-}		
isomers	E_{rel}	gap	NICS	E_{rel}	gap	NICS
I_h	0	1.94	9.99	0	0.97	−34.51
T_h(A)	−0.63	1.96	9.15	−0.52	0.97	−34.39
T_h(B)	−1.01	1.88	9.95			

Interestingly, we got the same hexaanion geometry for both T_h (A) and T_h (B). The energy sequence of B_{80}^{6-} parallels that of the neutral forms. Moreover, the hexaanions have comparable electronic configurations (Figure 1), which can be understood by the close similarity between the LUMOs of the neutral B_{80} cages.

For all the neutral B_{80} cages, the HOMOs mainly locate on the 6−6 bonds (bond shared by two hexagons), whereas the LUMOs prefer to be localized around the 5−6 bonds.[18b] In contrast, in the case of the B_{80} hexaanions, all the HOMOs and the LUMOs have bonding characteristics along the 5−6 bonds. Consequently, from the neutral forms to their hexaanions, the average 6−6 bond lengths increase by about 0.03 Å, while the average 5−6 bond lengths only increase less than 0.01 Å.

With 60 π electrons, B_{80} resembles C_{60}'s electron properties and is prone to accept six extra electrons.[19] It is well-known that C_{60} is weakly aromatic and C_{60}^{6-} is highly aromatic.[38] How will the extra electrons in B_{80} hexaanions affect the electron delocalization (aromaticity)? Is the 66-π-electron B_{80}^{6-} aromatic as C_{60}^{6-}? To answer these questions, we computed the NICS values at the cage centers of neutral B_{80} fullerenes and their hexaanions (Table 1). The neutral B_{80} cages are all weakly antiaromatic, as indicated by the moderately positive NICS values (ca. 10 ppm). In sharp contrast, their hexaanions with 66 π electrons are highly aromatic with rather negative NICS values (ca. −35 ppm). In comparison, the NICS value of C_{60}^{6-} is −50.0 ppm at the same theoretical level.[38d]

As pointed out by Chen et al.,[39] highly symmetrical aromatic cages are good hosts to encapsulate atoms to form stable clusters. Thus, B_{80}^{6-} structures are promising to enclose metal atoms or clusters, as in the case of C_{80} (I_h). This reveals a great possibility to design some energetically favorable endohedral borofullerenes by inserting into the B_{80} hollow cages some appropriate ions, which will play a role as electron donors.

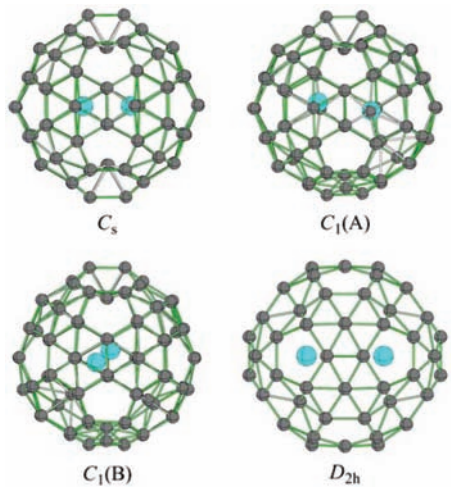

Figure 2. Four $La_2@B_{80}$ isomers optimized at the B3LYP/3-21G∼dz level of theory.

TABLE 2: Computed Geometric Parameters (Å), Relative Energies (E_{rel}, kcal/mol) and HOMO−LUMO Gap Energies (eV) of the Four $La_2@B_{80}$ Isomers at the B3LYP/3-21G∼dz Level of Theory

no.	isomer	R_{La-La}	R_{La-B}	E_{rel}	gap
1	C_s	3.34	2.69	0	1.32
2	C_1 (A)	3.31	2.80	6.46	1.34
3	C_1 (B)	3.37	2.70	33.57	1.21
4	D_{2h}	3.45	2.70	56.03	1.30

3.2. $La_2@B_{80}$ and $Sc_3N@B_{80}$. ***3.2.1. Optimized Geometries and Binding Energies.*** We explored four possible $La_2@B_{80}$ isomers by placing a La_2 pair along four different orientations with respect to the B_{80}^{6-} cage (the T_h (B) isomer was chosen as the initial geometry here). Full geometry optimizations were performed using the B3LYP/3-21G∼dz method, followed by harmonic frequency analysis at the same theoretical level. The optimized structures are all local minima with no imaginary frequencies (Figure 2).

Table 2 lists their La−La separations (R_{La-La}), the nearest La−B distance (R_{La-B}), relative energies, and gap energies. The calculated R_{La-La} values are 3.31−3.45 Å, apparently shorter than that in $La_2@C_{80}$ (ca. 3.7 Å).[26c] The C_s isomer has the lowest energy, closely followed by the C_1 (A) isomer, and the most unfavorable isomer (D_{2h}) is 56.03 kcal/mol higher in energy. Interestingly, the three lowest-energy isomers (i.e., the C_s isomer and two C_1 isomers, Figure 2) all have some boron atoms "dragged" toward the inner La_2 pair. For example, the nearest distance between the La atoms and the inward boron atoms is 3.03 Å for the C_s isomer. Note that all these *inward* boron atoms are *capping* atoms. This deviation is due to the rather strong interactions between the encapsulated metal atoms and the mobility of multicenter bonding characters of the capping boron atoms. To the best of our knowledge, this unusual cage distortion has not been observed for EMFs.

We followed the same computational procedure for $Sc_3N@B_{80}$. After full geometry optimization at the B3LYP/3-21G theoretical level, we got two local minima structures for $Sc_3N@B_{80}$ (Figure 3).

Table 3 lists their geometric parameters, relative energies, and HOMO−LUMO energy gaps. The nearest Sc−B distances (R_{Sc-B}) are 2.37 and 2.33 Å for the C_{2v} and the C_1 isomers, respectively. Energetically, the C_{2v} isomer is 14.75 kcal/mol lower than the C_1 isomer. The Sc_3N cluster in the C_{2v} isomer is planar, whereas that in the C_1 isomer is slightly distorted (the height from the N atom to the Sc_3 plane is ca. 0.2 Å). Note that some capping boron atoms deviate from the cage to the Sc_3N moiety. Not like $La_2@B_{80}$, however, these $Sc_3N@B_{80}$ isomers form one (C_1, the nearest N−B distance (R_{N-B}) is 1.43 Å) or two (C_{2v}, R_{N-B} is 1.57 Å) N−B covalent bonds. As a result, the N atoms are strongly absorbed by the outer cages, which differs significantly from the famous $Sc_3N@C_n$ family in which N is sitting at the center of (or slightly above) the Sc plane.[1,5,27] This can also be understood by the electron density analysis (see Section 3.2.2).

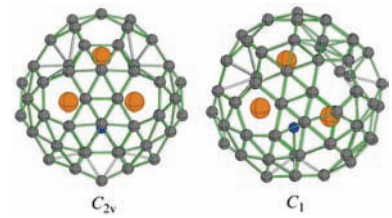

Figure 3. Two $Sc_3N@B_{80}$ isomers optimized at the B3LYP/3-21G level of theory.

TABLE 3: Computed Geometric Parameters (Å), Relative Energies (E_{rel}, kcal/mol), and HOMO−LUMO Gap Energies (eV) of the Two $Sc_3N@B_{80}$ Isomers at the B3LYP/3-21G Level of Theory

no.	isomer	R_{Sc-B}	R_{Sc-N}	R_{B-N}	E_{rel}	gap
1	C_{2v}	2.37	2.18	1.57	0	1.53
2	C_1	2.33	1.97	1.43	14.75	1.17

The favorable binding energies (154.8 and 514.7 kcal/mol, respectively, for the lowest-energy isomers, $La_2@B_{80}$ (C_s) and $Sc_3N@B_{80}$ (C_{2v})) indicate a considerable possibility to experimentally produce these endohedral complexes. Remarkably, the binding energy of $Sc_3N@B_{80}$ (C_{2v}) is even twice larger than that of the abundant $Sc_3N@C_{80}$ (247 kcal/mol).[40]

3.2.2. Electronic Properties. All the endohedral isomers have sizable HOMO−LUMO gap energies (ca. 1.2−1.3 eV for $La_2@B_{80}$, 1.17 and 1.53 eV for $Sc_3N@B_{80}$; Tables 2, 3), which suggests their high kinetic stabilities. Figure 4 displays the electron density in planes containing the inner ions for the lowest-energy isomers. No significant electron accumulation exists between the La/Sc ions and the B atoms, indicating an ionic character of the interaction. In contrast, the large electron density population between the N atom and two capping boron atoms illustrates the covalent bond character. The calculated Mulliken charge on each La ion, 3.65 *e*, reveals a plausible electron configuration of $(La^{3+})_2@B_{80}^{6-}$. A similar electron configuration ($(Sc_3N)^{6+}@B_{80}^{6-}$) can be assigned to $Sc_3N@B_{80}$.

The energy levels near the frontier molecular orbitals of the lowest-energy endohedral complexes were computed at the B3LYP/6-31G*∼dz level of theory, in comparison with the B_{80} T_h (B) isomer (Figure 5). Stuffing the metal atoms and the clusters into the B_{80} cage raises the HOMO levels (by 0.28 and 0.07 eV for $La_2@B_{80}$ and $Sc_3N@B_{80}$, respectively) while lowering the LUMO levels (by 0.28 and 0.35 eV for $La_2@B_{80}$ and $Sc_3N@B_{80}$, respectively). As a consequence, the gap energies of $La_2@B_{80}$ (C_s) and $Sc_3N@B_{80}$ are smaller by 0.56 and 0.42 eV than that of B_{80}, respectively. The La metal ions have very little contribution to the frontier orbitals, whereas the Sc ions play a substantial role in the LUMO (Figure 5, 6). As expected, the HOMOs of $La_2@B_{80}$ and $Sc_3N@B_{80}$ resemble that of B_{80}^{6-} very well.

To assist future experimental assignments, we calculated the vertical electron affinity (VEA) and vertical ionization potential

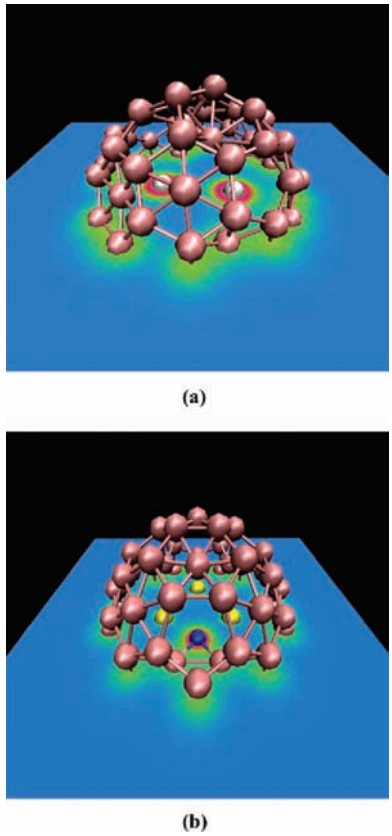

Figure 4. Electron density in planes passing through the inner ions of (a) the $La_2@B_{80}$ (C_s) and (b) the $Sc_3N@B_{80}$ (C_{2v}). The red and green colors represent high and low electron densities, respectively. The figure was generated with VMD 1.8.6.[41]

(VIP) as well as adiabatic electron affinity (AEA) and adiabatic ionization potential (AIP). The rather large electron affinities (VEA 2.76 eV, AEA 2.94 eV for $La_2@B_{80}$; VEA 2.88 eV, AEA 2.97 eV for $Sc_3N@B_{80}$) suggest that $La_2@B_{80}$ and $Sc_3N@B_{80}$ are likely good electron acceptors, whereas the high ionization potentials (VIP 6.14 eV, AIP 6.02 eV for $La_2@B_{80}$, VIP 6.40 eV, AIP 6.28 eV for $Sc_3N@B_{80}$) indicate that they are rather stable against oxidation.

3.2.3. Infrared and NMR Spectra. We also simulated the infrared (IR) and NMR spectra for the $La_2@B_{80}$ (C_s) and the $Sc_3N@B_{80}$ (C_{2v}) configurations (see the Supporting Information). The vibrational spectra for the T_h (B) B_{80} isomer previously simulated by Baruah et al.[18c] showed only several significant peaks. Sadrzadeh et al. analyzed the vibrational modes of this isomer and pointed out a radial breathing mode frequency of 474 cm^{-1} as a fingerprint.[19c]

With much lower symmetry, the C_s $La_2@B_{80}$ has a more complex IR spectrum, and all the 240 vibrational modes are IR-active (Figure 7a). The most intense absorption peak occurs at 1015 cm^{-1}. This vibrational mode (A') corresponds to the tangential motions of boron atoms on the cage surface. Several other relatively strong peaks are at 599, 608, 687, 802, 840, 890, and 1091 cm^{-1}. All the modes involving the heavy La ions correspond to the low-frequency peaks with rather small infrared intensities.

There are 246 vibrational modes for the $Sc_3N@B_{80}$ (C_{2v}), $67A_1 + 56A_2 + 61B_1 + 62B_2$, in which A_1, B_1, and B_2 are IR-active. Thus, ideally, up to 190 IR frequencies are measurable; however, the intensities of some of them are rather weak (Figure 7b). The strongest absorption peak at 710 cm^{-1} (A_1 mode) also corresponds to the tangential vibrations of boron

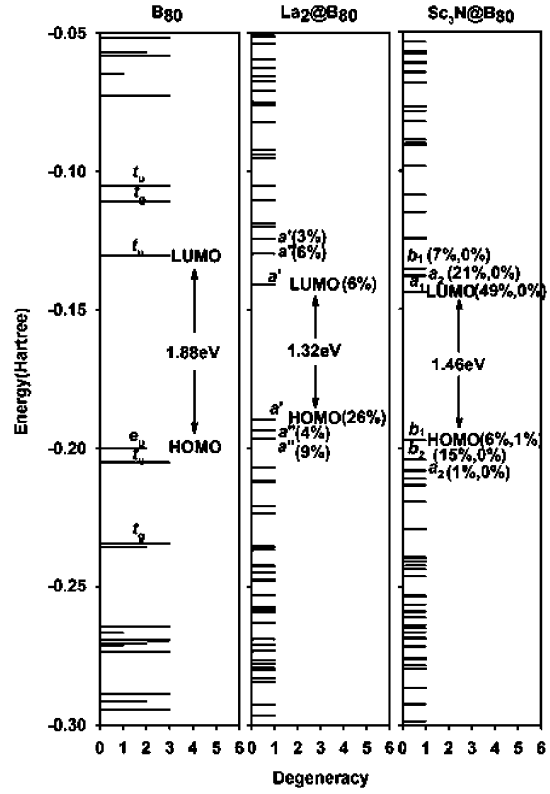

Figure 5. Energy levels near HOMO−LUMO gaps of the T_h (B) B_{80}, the $La_2@B_{80}$ (C_s) and the $Sc_3N@B_{80}$ (C_{2v}) computed at the B3LYP/6-31G*∼dz level of theory; La, Sc and N atoms' contributions to the orbitals are shown in parentheses.

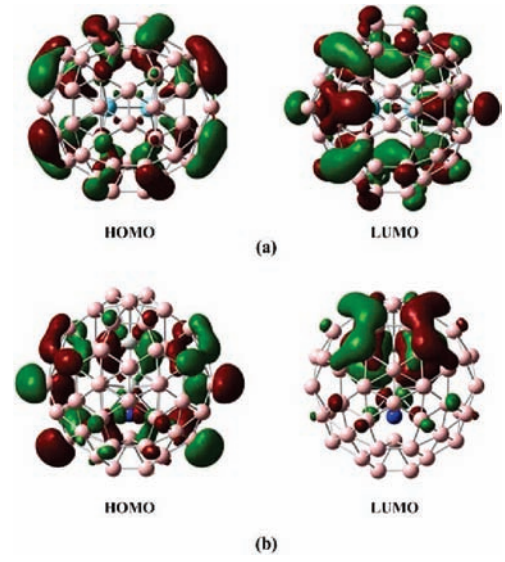

Figure 6. HOMO and LUMO of (a) the $La_2@B_{80}$ (C_s) and (b) the $Sc_3N@B_{80}$ (C_{2v}) isomers.

atoms along the cage surface as $La_2@B_{80}$. Several other expected strong peaks are at 583, 681, 836, 935, and 1065 cm^{-1}, respectively. The range from 600 to 1100 cm^{-1} is likely a characteristic for B_{80} endohedral complexes and may assist future experimental assignment.

^{11}B NMR will play a major role in the structural characterization of boron fullerenes and their derivatives. For the T_h (B) B_{80} and its hexaanion, the NMR lines are from 14.49 to 27.33 ppm and from −13.13 to −11.27 ppm, respectively. The $La_2@B_{80}$ (C_s) has 44 lines in observation, according to the C_s symmetry (Figure 8a), which range from −0.45 to 84.69 ppm.

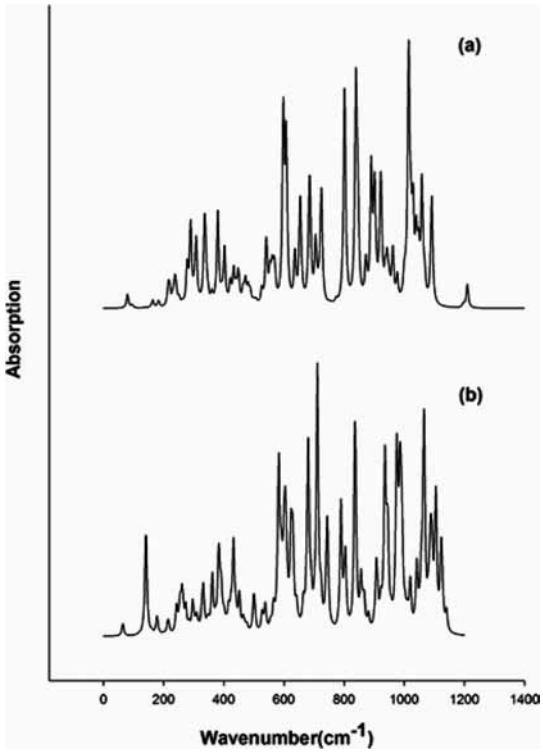

Figure 7. The calculated IR vibrational spectrum of (a) the $La_2@B_{80}$ (C_s) and (b) the $Sc_3N@B_{80}$ (C_{2v}) isomers.

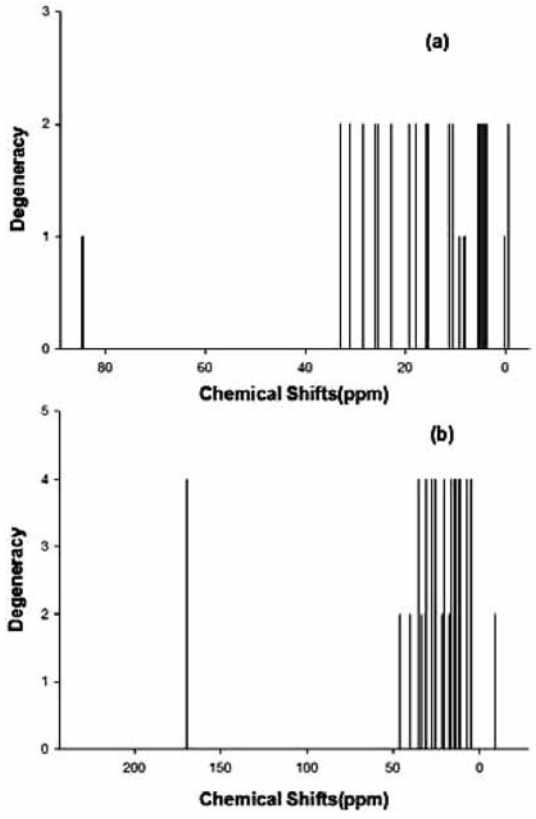

Figure 8. The calculated ^{11}B NMR of (a) the $La_2@B_{80}$ (C_s) and (b) the $Sc_3N@B_{80}$ (C_{2v}) isomers.

Note that the two peaks near 85 ppm (84.61 and 84.69 ppm) are well-separated far from other lines (by more than 50 ppm). These two peaks correspond to the two capping boron atoms in the σ_h symmetry plane and may serve as a fingerprint for future experimental spectroscopy characterization.

The $Sc_3N@B_{80}$ (C_{2v}) has 24 lines in the ^{11}B NMR spectrum, ranging from −9.18 to 169.45 ppm (Figure 8b). The 4-fold degenerate peak at 169.45 ppm, extremely far from other lines (by more than 120 ppm), corresponds to four capping boron atoms pulled toward the Sc_3N cluster. This ^{11}B shift is more deshielded than that in typical boranes, main-group heteroboranes, and substituted derivatives (the greatest ^{11}B chemical shift is 135.4 ppm in $B_4(^tBu)_4$).[42] The peak at −9.18 ppm corresponds to the two boron atoms in the B−N bonds. These two distinctive peaks may be utilized as fingerprints for experimental characterization.

Note that the $La_2@C_{80}$ and $Sc_3N@C_{80}$ cages have only one and two lines, respectively, in ^{13}C measurement due to the tumbling of the inner moiety.[43,44] Similar results may also be observed for $La_2@B_{80}$ and $Sc_3N@B_{80}$. Improved models should take the motions of the encapsulated atoms into account and involve NMR computations on various configurations.[45]

4. Conclusions

In summary, we predicted two representative endohedral metalloborofullerenes based on the B_{80} fullerene, $La_2@B_{80}$ and $Sc_3N@B_{80}$, by means of density functional computations. Their very favorable binding energies indicate their promise for experimental realization. The electronic and spectroscopy properties were simulated to assist future experimental characterization. We hope this work will stimulate more experimental and theoretical study on endohedral complexes of boron fullerenes.

Note Added in Proof. Very recently, several studies on boron fullerenes have been published.[46–50] Zope et al. proposed that infinite new members containing $32n^2$ or $80n^2$ atoms have high stability and can be added to the boron fullerene family.[46–47] Significantly, coated by Ca or Si atoms, B_{80} fullerenes were predicted to have considerable hydrogen storage capacity.[48–49]

Acknowledgment. This research has been supported in China by the National Natural Science Foundation of China (Grant no. 20773018) and in the U.S.A. by NSF Grant CHE-0716718, the Institute for Functional Nanomaterials (NSF Grant 0701525), and the U.S. Environmental Protection Agency (EPA Grant no. RD-83385601).

Supporting Information Available: The coordinates of the optimized endohedral complexes, detailed data for IR and NMR spectra as well as the full citation of ref 28. This material is available free of charge via the Internet at http://pubs.acs.org.

References and Notes

(1) For recent reviews, see (a) Akasaka, T.; Nagase, S. *Endofullerenes: A New Family of Carbon Clusters*; Kluwer Academic Publishers: New York, 2002. (b) Shinohara, N. *Rep. Prog. Phys.* **2000**, *63*, 843. (c) Guhaa, S.; Nakamotob, K. *Coord. Chem. Rev.* **2005**, *249*, 1111. (d) Dunsch, L.; Yang, S. *Electrochem. Soc. Interface* **2006**, *15*, 34. (e) Martin, N. *Chem. Commun.* **2006**, *2093*. (f) Dunsch, L.; Yang, S. *Small* **2007**, *3*, 1298. (g) Dunsch, L.; Yang, S. *Phys. Chem. Chem. Phys.* **2007**, *9*, 3067.

(2) (a) Kroto, H. W. *Nature* **1987**, *329*, 529. (b) Schmalz, T. G.; Seitz, W. A.; Klein, D. J.; Hite, G. E. *J. Am. Chem. Soc.* **1988**, *110*, 1113. (c) Fowler, P. W.; Manolopoulos, D. E. *An Atlas of Fullerenes*; Clarendon Press: Oxford, 1995.

(3) Campbell, E. E. B.; Fowler, P. W.; Mitchell, D.; Zerbetto, F. *Chem. Phys. Lett.* **1996**, *250*, 544.

(4) (a) Wang, C. R.; Kai, T.; Tomiyama, T.; Yoshida, T.; Kobayashi, Y.; Nishibori, E.; Takata, M.; Sakata, M.; Shinohara, H. *Nature* **2000**, *408*, 426. (b) Takata, M.; Nishibori, E.; Sakata, M.; Wang, C. R.; Shinohara, H. *Chem. Phys. Lett.* **2003**, *372*, 512.

(5) (a) Stevenson, S.; Fowler, P. W.; Heine, T.; Duchamp, J. C.; Rice, G.; Glass, T.; Harich, K.; Hajdu, E.; Bible, R.; Dorn, H. C. *Nature* **2000**, *408*, 427. (b) Olmstead, M. M.; Lee, H. M.; Duchamp, J. C.; Stevenson, S.; Marciu, D.; Dorn, H. C.; Balch, A. L. *Angew. Chem., Int. Ed.* **2003**, *42*, 900.

(6) Shi, Z. Q.; Wu, X.; Wang, C. R.; Lu, X.; Shinohara, H. *Angew. Chem., Int. Ed.* **2006**, *45*, 2107.

(7) Yang, S.; Popov, A. A.; Dunsch, L. *Angew. Chem., Int. Ed.* **2007**, *46*, 1256–1259.

(8) Wakahara, T.; Nikawa, H.; Kikuchi, T.; Nakahodo, T.; Rahman, G. M. A.; Tsuchiya, T.; Maeda, Y.; Akasaka, T.; Yoza, K.; Horn, E.; Yamamoto, K.; Mizorogi, N.; Slanina, Z.; Nagase, S. *J. Am. Chem. Soc.* **2006**, *128*, 14228.

(9) (a) Stevenson, S.; Burbank, P.; Harich, K.; Sun, Z.; Dorn, H. C.; van Loosdrecht, P. H. M.; de Vries, M. S.; Salem, J. R.; Kiang, C.-H.; Johnson, R. D.; Bethune, D. S. *J. Phys. Chem. A* **1998**, *102*, 2833. (b) Kato, H.; Taninaka, A.; Sugai, T.; Shinohara, H. *J. Am. Chem. Soc.* **2003**, *125*, 7782. (c) Lu, X.; Nikawa, H.; Nakahodo, T.; Tsuchiya, T.; Ishitsuka, M. O.; Maeda, Y.; Akasaka, T.; Toki, M.; Sawa, H.; Slanina, Z.; Mizorogi, N.; Nagase, S. *J. Am. Chem. Soc.* **2008**, *130*, 9129.

(10) Yamada, M.; Wakahara, T.; Tsuchiya, T.; Maeda, Y.; Akasaka, T.; Mizorogi, N.; Nagase, S. *J. Phys. Chem. A* **2008**, *112*, 7627.

(11) Yang, S.; Popov, A. A.; Dunsch, L. *J. Phys. Chem. B.* **2007**, *111*, 13659.

(12) Popov, A. A.; Krause, M.; Yang, S.; Wong, J.; Dunsch, L. *J. Phys. Chem. B* **2007**, *111*, 3363.

(13) Mercado, B. Q.; Beavers, C. M.; Olmstead, M. M.; Chaur, M. N.; Walker, K.; Holloway, B. C.; Echegoyen, L.; Balch, A. L. *J. Am. Chem. Soc.* **2008**, *130*, 7854.

(14) Beavers, C. M.; Zuo, T.; Duchamp, J. C.; Dorn, H. C.; Olmstead, M. M.; Balch, A. L. *J. Am. Chem. Soc.* **2006**, *128*, 11352.

(15) Zuo. T.; Walker, K.; Olmstead, M. M.; Melin, F.; Holloway, B. C.; Echegoyen, L.; Dorn, H. C.; Chaur, M. N.; Chancellor, C. J.; Beavers, C. M.; Balch, A. L.; Athans. A. J. *Chem. Commun.* **2008**, *1067*.

(16) Alexandrova, A. N.; Boldyrev, A. I.; Zhai, H.; Wang, L. *Coord. Chem. Rev.* **2006**, *250*, 2811–2866.

(17) Szwacki, N. G.; Sadrzadeh, A.; Yakobson, B. I. *Phys. Rev. Lett.* **2007**, *98*, 166804.

(18) (a) Szwacki, N. G.; Sadrzadeh, A.; Yakobson, B. I. *Phys. Rev. Lett.* **2008**, *100*, 159901. (b) Gopakumar, G.; Nguyen, M. T.; Ceulemans, A. *Chem. Phys. Lett.* **2008**, *450*, 175. (c) Baruah, T.; Pederson, M. R.; Zope, R. R. *Phys. Rev. B* **2008**, *78*, 045408.

(19) (a) Prasad, D. L. V. K.; Jemmis, E. D. *Phys. Rev. Lett.* **2008**, *100*, 165504. (b) Ceulemans, A.; Muya, J. T.; Gopakumar, G.; Nguyen, M. T. *Chem. Phys. Lett.* **2008**, *461*, 226. (c) Sadrzadeh, A.; Pupysheva, O. V.; Singh, A. K.; Yakobson, B. I. *J. Phys. Chem. A* **2008**, *112*, 13679.

(20) Tang, H.; Ismail-Beigi, S. *Phys. Rev. Lett.* **2007**, *99*, 115501.

(21) Yang, X.; Ding, Y.; Ni, J. *Phys. Rev. B* **2008**, *77*, 041402(R).

(22) Yan, Q.; Zheng, Q.; Su, G. *Phys. Rev. B* **2008**, *77*, 224106.

(23) Liu, A. Y.; Zope, R. R; Pederson, M. R. *Phys. Rev. B* **2008**, *78*, 155422.

(24) Li, Y.; Zhou, G.; Li, J.; Gu, B.; Duan, W. *J. Phys. Chem. C* **2008**, *112*, 19268.

(25) (a) Szwacki, N. G. *Nanoscale Res. Lett.* **2008**, *3*, 49. (b) Yan, Q.; Sheng, X.; Zheng, Q.; Zhang, Li.; Su, G. *Phys. Rev. B* **2008**, *78*, 201401(R.

(26) (a) Suzuki, T.; Maruyama, Y.; Kato, T.; Kikuchi, K.; Nakao, Y.; Achiba, Y.; Kobayashi, K.; Nagase, S. *Angew. Chem., Int. Ed. Engl.* **1995**, *34*, 1094. (b) Akasaka, T.; Nagase, S.; Kobayashi, K.; Walchli, M.; Yamamoto, K.; Funasaka, H.; Kako, M.; Hoshino, T.; Erata, T. *Angew. Chem., Int. Ed. Engl.* **1997**, *36*, 1643. (c) Shimotani, H.; Ito, T.; Iwasa, Y.; Taninaka, A.; Shinohara, H.; Nishibori, E.; Takata, M.; Sakata, M. *J. Am. Chem. Soc.* **2004**, *126*, 364.

(27) Stevenson, S.; Rice, G.; Glass, T.; Harich, K.; Cromer, F.; Jordan, M. R.; Craft, J.; Hadju, E.; Bible, R.; Olmstead, M. M.; Maitra, K.; Fisher, A. J.; Balch, A. L.; Dorn, H. C. *Nature* **1999**, *401*, 55.

(28) Frisch, M. J. et al., *Gaussian 03*, Gaussian, Inc., Wallingford CT, 2004. See the Supporting Information for the full reference.

(29) (a) Becke, A. D. *J. Chem. Phys.* **1993**, *98*, 5648. (b) Lee, C.; Yang, W.; Parr, R. G. *Phys. Rev. B* **1988**, *37*, 785.

(30) Hehre, W. J.; Ditchfield, R.; Pople, J. A. *J. Chem. Phys.* **1972**, *56*, 2257.

(31) Binkley, J. S.; Pople, J. A.; Hehre, W. J. *J. Am. Chem.Soc.* **1980**, *102*, 939.

(32) Hay, P. J.; Wadt, W. R. *J. Chem. Phys.* **1985**, *82*, 299.

(33) von Ragué Schleyer, P.; Maerker, C.; Dransfeld, A.; Jiao, H.; van Eikema Hommes, N. J. R. *J. Am. Chem. Soc.* **1996**, *118*, 6317.

(34) See reviews: (a) Chen, Z.; Heine, T.; von Ragué Schleyer, P.; Sundholmd, D. In *Calculation of NMR and EPR Parameters. Theory and Applications*; Kaupp, M., Bühl, M., Malkin, V. G., Eds.; Wiley-VCH: New York, 2004; p395. (b) Chen, Z.; Wannere, C. S.; Corminboeuf, C.; Puchta, R.; von Ragué Schleyer, P. *Chem. Rev* **2005**, *10*, 3842.

(35) Wolinski, K.; Hilton, J. F.; Pulay, P. *J. Am. Chem. Soc.* **1990**, *112*, 8251.

(36) Mennekes, T.; Paetzold, P.; Boese, R.; Bläser, D. *Angew. Chem., Int. Ed. Engl.* **1991**, *30*, 173.

(37) Sternfeld, T.; Thilgen, C.; Chen, Z.; Siefken, S.; von Ragué Schleyer, P.; Thiel, W.; Diederich, F.; Rabinovitz, M. *J. Org. Chem.* **2003**, *68*, 4850.

(38) (a) Saunders, M.; Jiménez-Vázquez, H. A.; Cross, R. J.; Mroczkowski, S.; Freedberg, D. I.; Anet, F. A. L. *Nature* **1994**, *367*, 256. (b) Bühl, M.; Thiel, W.; Jiao, H.; von Ragué Schleyer, P.; Saunders, M.; Anet, F. A. L. *J. Am. Chem. Soc.* **1994**, *116*, 6005. (bb) Bühl, M.; Hirsch, A. *Chem Rev* **2001**, *101*, 1153, and references therein. (d) Chen, Z.; King, R. B. *Chem. Rev.* **2005**, *105*, 3613.

(39) Chen, Z.; Neukermans, S.; Wang, X.; Janssens, E.; Zhou, Z.; Silverans, R. E.; King, R. B.; von Ragué Schleyer, P.; Lievens, P. *J. Am. Chem. Soc.* **2006**, *128*, 12829.

(40) Kobayashi, K.; Sano, Y.; Nagase, S. *J. Comput. Chem.* **2001**, *22*, 1353.

(41) Humphrey, W.; Dalke, A.; Schulten, K. *J. Mol. Graphics* **1996**, *14*, 33.

(42) Heřmánek, S. *Chem. Rev.* **1992**, *92*, 325.

(43) Akasaka, T.; Nagase, S.; Kobayashi, K.; Wälchli, M.; Yamamoto, K.; Funasaka, H.; Kako, M.; Hoshino, T.; Erata, T. *Angew. Chem., Int. Ed. Engl.* **1997**, *36*, 1643.

(44) Stevenson, S.; Rice, G.; Glass, T.; Harich, K.; Cromer, F.; Jordan, M. R.; Craft, J.; Hadju, E.; Bible, R.; Olmstead, M. M.; Maitra, K.; Fisher, A. J.; Balch, A. L.; Dorn, H. C. *Nature (London)* **1999**, *401*, 55.

(45) Heine, T.; Vietze, K.; Seifert, G. *Magn. Reson. Chem.* **2004**, *42*, S199.

(46) Zope, R. R.; Baruah, T.; Lau, K. C.; Liu, A. Y.; Pederson, M. R.; Dunlap, B. I. *Phys. Rev. B* **2009**, *79*, 161403(R).

(47) Zope, R. R. *Europhys. Lett.* **2009**, *85*, 68005.

(48) Wu, G.; Wang, J.; Zhang, X.; Zhu, L. *J. Phys. Chem. C* **2009**, *113*, 7052.

(49) Li, M.; Li, Y.; Zhou, Z.; Shen, P.; Chen, Z. *Nano Lett.* **2009**, *9*, 1944.

(50) Botti, S.; Castro, A.; Lathiotakis, N. N.; Andrade, X.; Marques, M. A. L. *Phys. Chem. Chem. Phys.* **2009**, *11*, 4523.

JP9019848